Am J Nucl Med Mol Imaging 2017;7(2):40-52
www.ajnmmi.us /ISSN:2160-8407/ajnmmi0046734

Original Article

Synthesis and evaluation of [^{64}Cu]PSMA-617 targeted for prostate-specific membrane antigen in prostate cancer

Can Cui[1*], Masayuki Hanyu[2*], Akiko Hatori[2], Yiding Zhang[2], Lin Xie[2], Tomoya Ohya[2], Masami Fukada[2], Hisashi Suzuki[2], Kotaro Nagatsu[2], Cuiping Jiang[1], Rui Luo[1], Guoqiang Shao[1], Mingrong Zhang[2], Feng Wang[1]

[1]Department of Nuclear Medicine, Nanjing First Hospital, Nanjing Medical University, Nanjing, China; [2]Department of Radiopharmaceutics Development, National Institute of Radiological Sciences, National Institutes for Quantum and Radiological Science and Technology, Chiba, Japan. [*]Equal contributors.

Received August 29, 2016; Accepted January 5, 2017; Epub April 15, 2017; Published April 30, 2017

Abstract: We radiolabeled a ligand, PSMA-617, of prostate-specific membrane antigen (PSMA) with copper-64 (^{64}Cu), to evaluate the metabolism, biodistribution, and potential of [^{64}Cu]PSMA-617 for PET imaging of prostate cancer. [^{64}Cu]PSMA-617 was synthesized by heating PSMA-617 with [^{64}Cu]$CuCl_2$ in buffer solution at 90°C for 5 min. *In vitro* uptake was determined in two cell lines of prostate cancer. *In vivo* regional distributions were determined in normal and tumor-bearing mice. High radiolabeling efficiency of ^{64}Cu for PSMA-617 yielded [^{64}Cu]PSMA-617 with >99% radiochemical purity. *In vitro* cellular uptake experiments demonstrated the specificity of [^{64}Cu]PSMA-617 for PSMA-positive LNCaP cells. Biodistribution observations of normal mice revealed high uptake of radioactivity in the kidney and liver. PET with [^{64}Cu]PSMA-617 visualized tumor areas implanted by PSMA-positive LNCaP cells in the mice. Two hours after the injection of [^{64}Cu]PSMA-617 into mice, a radiolabeled metabolite was observed in the blood, liver, urine, and LNCaP tumor tissues. [^{64}Cu]PSMA-617 was easily synthesized, and exhibited a favorable biodistribution in PSMA-positive tumors. Although this radioligand shows slow clearance for kidney and high liver uptake, change of its chelator moiety and easy radiolabeling may enable development of new ^{64}Cu or ^{67}Cu-labeled PSMA ligands for imaging and radiotherapy.

Keywords: Prostate-specific membrane antigen, ^{64}Cu, PSMA-617, [^{64}Cu]PSMA-617

Introduction

In western societies, prostate cancer (PCa) is the most common cancer in elderly men and the third most frequent cause of cancer-related mortality: PCa and its complications kill more than 200,000 peoples annually [1, 2]. Innovative diagnostic methods, especially in magnetic resonance imaging, have improved the specificity and sensitivity of PCa diagnosis. However, detecting lymph metastasis noninvasively remains challenging. Nowadays, lymph node dissection is the only reliable staging method [3].

Prostate specific membrane antigen (PSMA) is a type II glycoprotein with an extensive extracellular domain (44-750 amino acids); this protein plays a significant role in prostate carcinogenesis and progression [4]. PSMA restricts its expression to the surface of PCa, particularly in androgen-independent, advanced, and metastatic disease. Low-level PSMA expression occurs in primary renal tumors and transitional cell carcinoma of the bladder [5, 6]. PSMA is also expressed within the endothelium of most solid tumors [7].

PSMA was identified as the antigen of the monoclonal antibody 7E11-C5. Indium-111 (^{111}In)-labeled 7E11-C5 recognizes the intracellular domain of PSMA; this radiolabelled antibody (commercially known as ProstaScint) is a radiopharmaceutical for the PSMA-targeted treatment of PCa [8]. In addition, radiolabelled huJ591, an antibody labeled with yttrium-90, ^{111}In, or lutetium-177 (^{177}Lu) that recognizes the extracellular portion of PSMA, was successfully

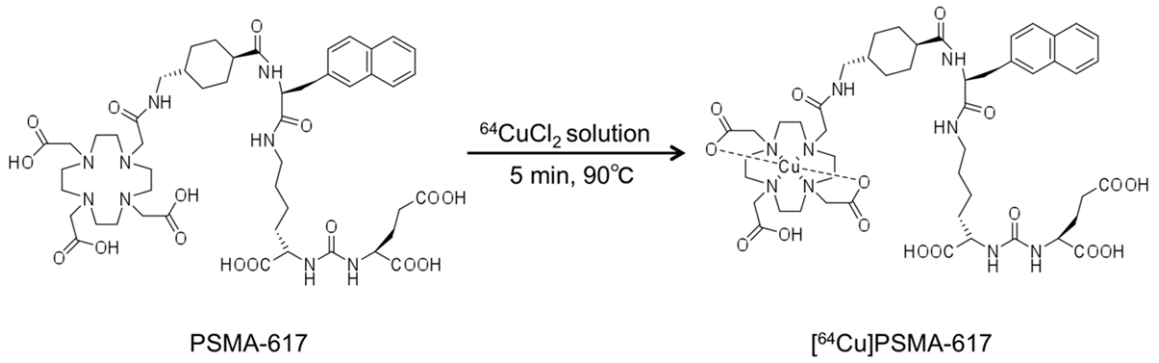

Figure 1. Synthesis of [^{64}Cu]PSMA-617 from PSMA-617 and [^{64}Cu]$CuCl_2$.

translated into clinical trials [9]. However, because the large sizes of 7E11-C5 and huJ591 tend to prolong clearance, access to all of the tumor portions is typically restricted, especially for viable cells with intact membranes.

Radioligands with low molecular weights often exhibit imaging pharmacokinetics superior to those of radiolabeled antibodies, due to relatively short circulation times and rapid clearance from non-target tissues. A variety of low-molecular-weight PCa-imaging radioligands have been developed [10-12]. Among them, radiolabeled urea-based PSMA inhibitors were found to be useful for imaging or radiotherapy of PCa [13-16]. Recently, 2-[3-(1-carboxy-5-{3-naphthalen-2-yl-2-[(4-{[2-(4,7,10-tris-carboxymethyl-1,4,7,10-tetraazacyclododec-1-yl)acetylamino]methyl}cyclohexanecarbonyl)amino]propionylamino}pentyl)ureido]- pentanedioic acid (PSMA-617), Glu-urea-Lys-2-naphtyl-L-Ala-cyclohexane conjugated with 1,4,7,10-tetraazacyclododecane-N,N',N,N'-tetraacetic acid (DOTA), has been developed as a novel PSMA ligand [17, 18]. The PSMA-617 radioligand labeled with gallium-68 (^{68}Ga), scandium-44, ^{177}Lu, or ^{111}In exhibits significant benefits in biodistribution and efficiency towards solid tumor in mice and humans [17-22].

In the present study, we sought to label PSMA-617 with copper-64 (^{64}Cu), and to evaluate the potential of [^{64}Cu]PSMA-617 (**Figure 1**) as a PET ligand for imaging PSMA in PCa. ^{64}Cu-labeled ligands are useful in PET studies because of the clinically suitable nuclear properties of ^{64}Cu ($t_{1/2}$ = 12.7 h, β^+ 17.4%, Emax = 0.656 MeV, β^- 39%, Emax = 0.573 MeV) and its availability at high specific activity. The longer physical half-life of ^{64}Cu relative to conventional carbon-11 and fluorine-18 enables imaging at delayed time points. This property allows sufficient time for clearance of non-specific radioactivity from background tissues to increase image contrast, particularly for antibodies and nanoparticles, which require long times to circulate throughout the whole body [23]. Moreover, ^{64}Cu-labeled ligands are demonstrably effective for radioimmunotherapy [23].

In this study, we radiosynthesized [^{64}Cu]PSMA-617 for the first time. We performed metabolite analysis, biodistribution studies, and PET scans of normal and tumor-bearing mice using this radioligand. The specificity of [^{64}Cu]PSMA-617 for LNCaP was demonstrated in the tumor cells and the tumor-bearing mice.

Materials and methods

PSMA-617 was purchased from ABX (Radeberg, Germany). All chemicals were from Wako Pure Chemical Industries (Osaka, Japan) and Sigma-Aldrich (St. Louis, MI, USA). ^{64}Cu was produced at the National Institute of Radiological Science (Chiba, Japan) with 98% radionuclidic purity [24]. All radio-HPLC analysis for [^{64}Cu]PSMA-617 was performed using a JASCO HPLC system (JASCO, Tokyo, Japan) coupled with an X-Terra C-18 column (4.6 mm i.d. × 150 mm, 5 μm, Waters, Milford, MA, USA). A flow rate of 1 mL/min was used with a linear mobile phase gradient. The gradient started with 90% solvent A (0.1% trifluoroacetic acid [TFA] in water) and 10% solvent B (0.1% TFA in acetonitrile [MeCN]), and 10 min later, ended with 0% solvent A and 100% solvent B. Effluent radioactivity was measured using a NaI (Tl) scintillation detector system (Ohyo Koken Kogyo, Tokyo, Japan). A 1480 Wizard autogamma counter (PerkinElmer,

Waltham, MA, USA) was used to measure radioactivity, as expressed in counts of radioactivity per minute (cpm), accumulating in cells and animal tissues. A dose calibrator (IGC-7 Curiemeter; Aloka, Tokyo, Japan) was used for the other radioactivity measurements.

Preparation of [^{64}Cu]PSMA-617

We mixed 10 μL each of PSMA-617 (5 nmol, 0.5 mM in 0.1 M ammonium citrate buffer [pH = 5.5]) with [^{64}Cu]$CuCl_2$ (37-222 MBq, 3.7-22.2 MBq/μL in the same buffer). The reaction mixture was heated at 90°C for 5 min. The radiolabeling efficiency and radiochemical purity were analyzed using reversed-phase HPLC. The specific activity of [^{64}Cu]PSMA-617 was calculated by comparing the obtained radioactivity to the total mass of PSMA-617 used for labeling. To determine the radiochemical stability, the product was incubated at 37°C for 24 h, and its radiochemical purity was subsequently analyzed by radio-HPLC.

Cell line and animals

Two human prostate carcinoma cell lines, LNCaP (PSMA-positive) and PC-3 (PSMA-negative), were used in the present study. Both cell lines were maintained and passaged in a humidified CO_2 incubator (37°C/5% CO_2). LNCaP (RIKEN BRC Cell Bank, Ibaraki, Japan) was maintained and passaged in RPMI 1640 medium containing 4.5 g/L glucose with 10% fetal bovine serum. PC-3 (JCRB Cell Bank, Osaka, Japan) was maintained and passaged in Ham's F-12K medium with 8% fetal bovine serum. Both media were supplemented with antibiotics (penicillin/streptomycin).

Male BALB/c *nu/nu* mice and ICR mice (7 week old) were purchased from Japan SLC (Shizuoka, Japan). All animals received humane care, and the Animal Ethics Committee of the National Institute of Radiological Sciences approved all experiments. All experiments were carried out according to the recommendations of the Committee for the Care and Use of Laboratory Animals, National Institute of Radiological Sciences.

Tumor-bearing models using BALB/c *nu/nu* mice were prepared via a left flank subcutaneous injection of 100 μL of an 1:1 mixture of LNCaP cell suspension and Matrigel basement membrane matrix (5×10^6 cells/mouse; Becton Dickinson, Franklin Lakes, NJ, USA). Ten days later, PC-3 cell suspension was injected into the right flank (7×10^6 cells/mouse). Tumor-bearing mice were used for studies when tumor diameters reached 5-10 mm.

Cellular uptake and inhibion experiment

PC-3 and LNCaP cells in 24-well plates (1×10^5 cells/well) were maintained for 48 h (37°C/5% CO_2). The medium was removed, and each well was washed three times with phosphate buffered saline (PBS). [^{64}Cu]PSMA-617 in medium (74 kBq/1 mL) was added to each well, and the plates were incubated at 37°C for 5 min, 1 h, and 2 h. After incubation, the reaction solution was removed, and each well was washed three times with PBS and the cells were lysed with 0.5 mL NaOH (0.2 mol/L). Radioactivity in cell lysate was measured with the autogamma counter. The protein content of cell lysate was quantified using a Bio-Rad protein assay kit (Bio-Rad, Hercules, CA, USA). Cellular uptake was calculated as a percentage of incubated radioactivity per milligrams of protein.

Binding inhibition assay was performed using LNCaP cells. PSMA-617 (final concentration: 0, 0.2, 2, 20, 200, or 2000 nmol/L) and [^{64}Cu]PSMA-617 (74 kBq/1 mL) in medium were added to each well, and the plates were incubated at 37°C for 1 h. After the incubation, cells were treated as they had been for the *in vitro* uptake assay. Specific binding was calculated by subtracting nonspecific binding (residual binding of radioligand in presence of 2 μmol/L of unlabeled PSMA-617) from total binding (without addition of unlabeled PSMA-617).

Metabolite analysis

ICR mice (n = 3 for each time point) were sacrificed by cervical dislocation at 1 h and 2 h after the injection of [^{64}Cu]PSMA-617 (3.7 MBq/200 μL). At each time point, the blood and urine samples were quickly obtained by cardiac and urinary bladder puncture from each mouse. Also liver sample was removed quickly. Each urine or blood sample was collected in a test tube containing acetonitrile/water (1:1, 500 μL). The mixture was vortexed, and subsequently centrifuged at 15000 rpm for 15 min. Liver sample was homogenized in an ice-cooled acetonitrile/H_2O solution (1:1, 2 mL) using a

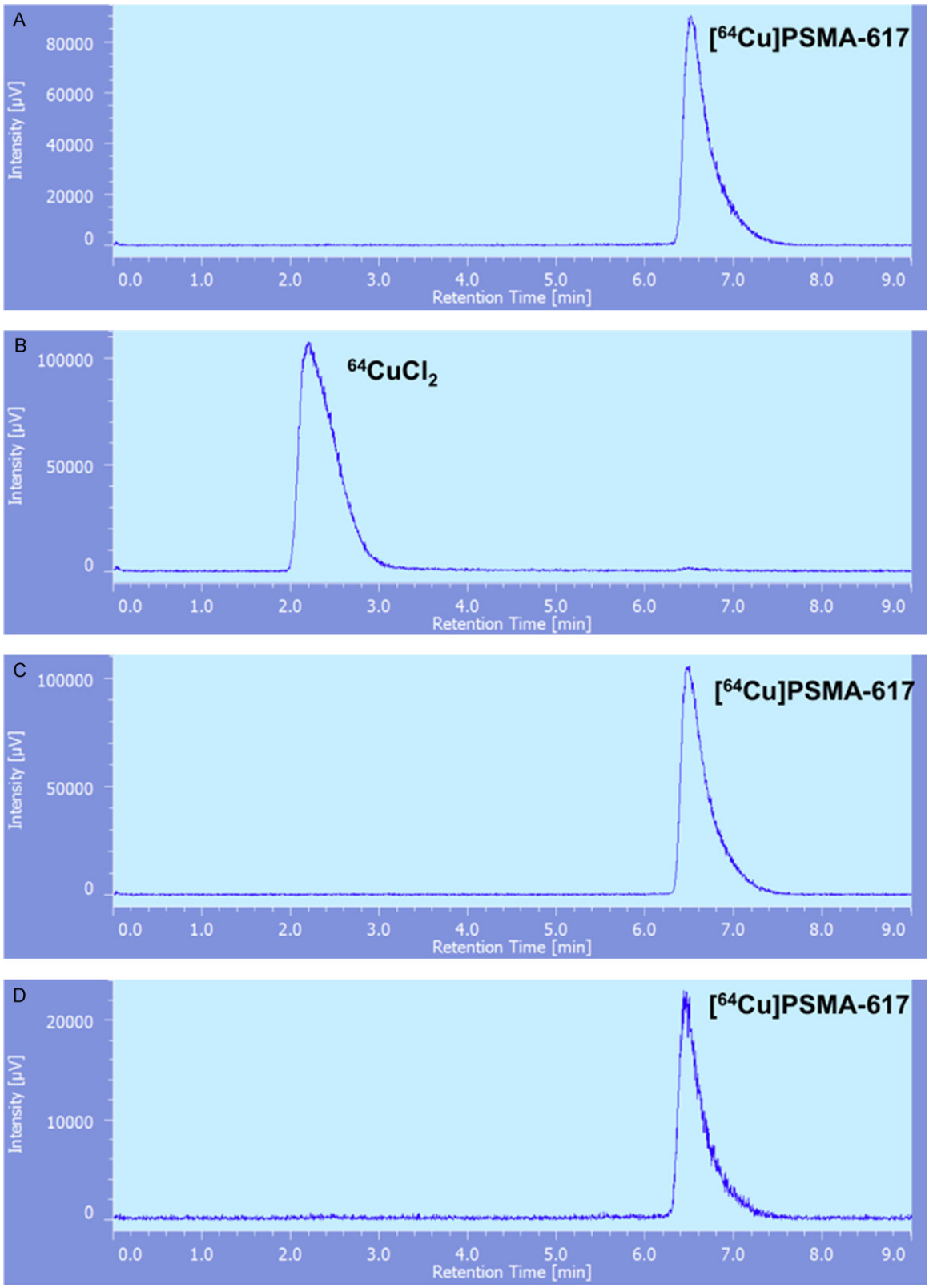

Figure 2. Analytical radio-HPLC chromatograms of (A) [^{64}Cu]PSMA-617 yielded from radiolabeling 20 nmol PMSA-617; (B) [^{64}Cu]$CuCl_2$ as a comparison; (C) [^{64}Cu]PSMA-617 yielded from radiolabeling 5 nmol PSMA-617; (D) Radiochemical stability of [^{64}Cu]PSMA-617 after 24 h incubation at 37 °C.

Silent Crusher S homogenizer, and centrifuged at 15000 rpm for 15 min. The supernatant of each sample was collected, mixed with an equal volume of acetonitrile, and centrifuged again at the same conditions for 20 min. An aliquot of the supernatant (0.1-1.0 mL) obtained from the urine, blood, or liver homogenate was injected into the HPLC system and analyzed. The percentage ratio of [^{64}Cu]PSMA-617 (t_R = 6.2-6.4 min) to total radioactivity on the HPLC chromatogram was calculated as % = (peak area for [^{64}Cu]PSMA-617/total peak area) × 100.

To examine the metabolite of [^{64}Cu]PSMA-617 in LNCaP tumor, the tumor-bearing mice (n = 3) were sacrificed by cervical dislocation at 2 h after the injection of [^{64}Cu]PSMA-617 (17 MBq/100 μL). The LNCaP tumor tissues were cut from the mice and treated as above.

Biodistribution

A saline solution of [^{64}Cu]PSMA-617 (0.74 MBq/200 μL) was injected into ICR mice via the tail vein. Four mice were sacrificed by cervical dislocation at 0.5, 1, 2, 12, and 24 h after injection. Major organs, including the heart, liver, lung, spleen, pancreas, kidneys, stomach, duodenum (including contents), muscle, and blood were quickly harvested and weighed. The radioactivity in these organs was measured using the autogamma counter. The results are expressed as the percentage of injected dose per gram of wet tissue (% ID/g). All radioactivity measurements were decay-corrected.

Small-animal PET study

PET scans were conducted using an Inveon PET scanner (Siemens Medical Solutions, Knoxville, TN, USA), which provides 159 transaxial slices with 0.796-mm (center-to-center) spacing, a 10-cm transaxial field of view, and a 12.7-cm axial field of view. Normal ICR and tumor-bearing BALB/c *nu/nu* mice were kept in the prone position under anesthesia with 1-2% (v/v) isoflurane during the scan. [^{64}Cu]PSMA-617 (7-17 MBq/100 μL) was injected via a preinstalled tail vein catheter. Immediately after the injection, a dynamic scan in 3D list mode was acquired for 60 min (ICR normal mice, n = 6; tumor-bearing mice, n = 6). Maximum intensity projection (MIP) images were obtained for ICR normal and tumor-bearing mice, respectively. PET dynamic images were reconstructed by filtered back projection using Hanning's filter with a Nyquist cutoff of 0.5 cycle/pixel, which were summed using analysis software (ASIPro VM, Siemens Medical Solutions). Volumes of interest, including the heart, kidneys, liver, lung, bone, and tumors, were placed using the ASIPro software. The radioactivity was decay-corrected for the injection time and expressed as the standardized uptake value (SUV). SUV = (radioactivity per mL tissue/injected radioactivity) × body weight.

Immunohistochemical staining assay

After the tumor-bearing mice were sacrificed, tumors, liver, and kidney were quickly harvested and frozen. Frozen samples were cut in-house into 5-μm-thick slices, using a cryotome (HM560, Carl Zeiss, Oberkochen, Germany). Sections were fixed with cold acetone and dried. After washing with PBS, the sections were incubated with rabbit anti PSMA antibody (1:400, Cell Signaling Technology, Danvers, MA, USA) overnight at 4°C. Following the first immunoreaction, the sections were incubated with fluorophore-conjugated goat anti-rabbit IgG secondary antibody (1:500; Invitrogen, Camarillo, CA, USA) for 1 h at room temperature. The sections were washed with PBS and mounted using ProLong Gold Antifade Mountant with DAPI (Life Technologies, Eugene, OR, USA). Fluorescent images were captured using a fluorescence microscope (BZ-9000, Keyence, Osaka, Japan).

Statistics

All measurements are expressed as means ± standard deviations (SD). Statistical analyses were performed using the GraphPad Prism 5 software (GraphPad Software, La Jolla, CA, USA).

Results and discussion

Radiochemistry

Radioligand [^{64}Cu]PSMA-617 was synthesized by labeling PSMA-617 with [^{64}Cu]$CuCl_2$ in buffer solution (**Figures 1** and **2**). PSMA-617 (20 nmol) with ^{64}Cu exhibited >99% radiolabeling efficiency at 90°C for 30 min, as shown in the radio-HPLC chromatogram for the reaction mixture (**Figure 2A**). The retention time (t_R) of [^{64}Cu]

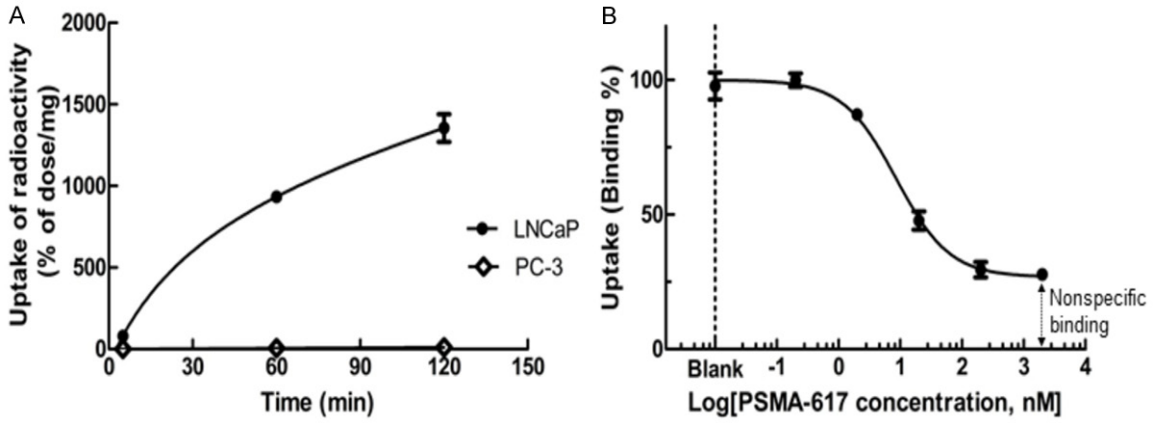

Figure 3. A: Uptake of [^{64}Cu]PSMA-617 into LNCaP and PC-3 cells. B: Inhibition curve for the uptake of [^{64}Cu]PSMA-617 by LNCaP cells at various concentrations of unlabeled PSMA-617; a nonlinear regression curve fit the data with R^2 = 0.9794.

PSMA-617 was 6.4 min, while that of free [^{64}Cu] Cu^{2+} as a comparison was 2 min (**Figure 2B**). Decreasing the reaction time to 10 min also achieved the same labeling efficiency. To minimize the influence of unreacted PSMA-617 on the binding and imaging experiments as much as possible, the amount of PSMA-617 used was optimized for radiolabeling. When the amount of PSMA-617 was decreased to 5 nmol, a 10 min radiolabeling reaction achieved >99% efficiency. Even when the reaction was performed for 5 min at 90°C (**Figure 2C**) or room temperature, the efficiencies also remained at 99%. However, when the amount of PSMA-617 was further decreased to 1 nmol, the labeling efficiency was reduced to 90%. Reactions of 1 nmol PSMA-617 performed for 5 min at 90°C or room temperature only attained markedly reduced efficiencies.

After optimizing the reaction conditions, radiolabeling was carried out with the use of 5 nmol PSMA-617 at 90°C for 5 min to produce [^{64}Cu] PSMA-617 with the best labeling efficiency. Because of this reaction's efficiency and low amount of PSMA-617 used, the desired product was directly obtained from the reaction mixture without purification. This labeling experiment started with 222 MBq [^{64}Cu]$CuCl_2$ solution and yielded ~ 200 MBq [^{64}Cu]PSMA-617 (n = 6) as an animal-injectable solution. In the final product, we did not find significant peak of unreacted [^{64}Cu]Cu^{2+}. The specific activity of [^{64}Cu]PSMA-617 was estimated to be 8.0-48.1 GBq/μmol. At 24 h after retaining this product at 37°C, its radiochemical purity remained greater than 95% (**Figure 2D**). This product did not exhibit radiolysis, indicating its radiochemical stability for at least one day. The analytical results of [^{64}Cu]PSMA-617 were in compliance with our in-house quality control/assurance specifications for radiopharmaceuticals.

In vitro uptake into LNCaP and PC-3 cells

Figure 3A shows *in vitro* uptakes of [^{64}Cu] PSMA-617 into PSMA-positive LNCaP and PSMA-negative PC-3 cell lines. These two PCa cell lines are used often for PSMA studies [25]. When exposed to LNCaP cells, [^{64}Cu]PSMA-617 started to accumulate into these cells (80.1 ± 6.4% of dose/mg at 5 min after the incubation); the radioactivity level had increased to 1355.0 ± 170.2% of dose/mg by 2 h. On the other hand, the uptake of [^{64}Cu]PSMA-617 by PC-3 was only 0.7 ± 0.2% of dose/mg at 5 min after the incubation, and 11.5 ± 2.1% of dose/mg at 2 h. Protein amounts were measured 0.071 ± 0.008 mg/well for LNCaP, and 0.076 ± 0.002 mg/well for PC-3 cells. At corresponding time points, the PC-3 cell uptakes were significantly lower than the LNCaP uptake values ($P<0.0001$).

To confirm the specific binding of [^{64}Cu]PSMA-617 to PSMA, unlabeled PSMA-617 at various concentrations was used to carry out inhibition experiments for the uptake of radioactivity in the PSMA-positive LNCaP cells at 60 min after the incubation (**Figure 3B**). Addition of unlabeled PSMA-617 reduced the uptake of [^{64}Cu] PSMA-617 in a dose-dependent order. Specific binding amounted to about 73% of total radio-

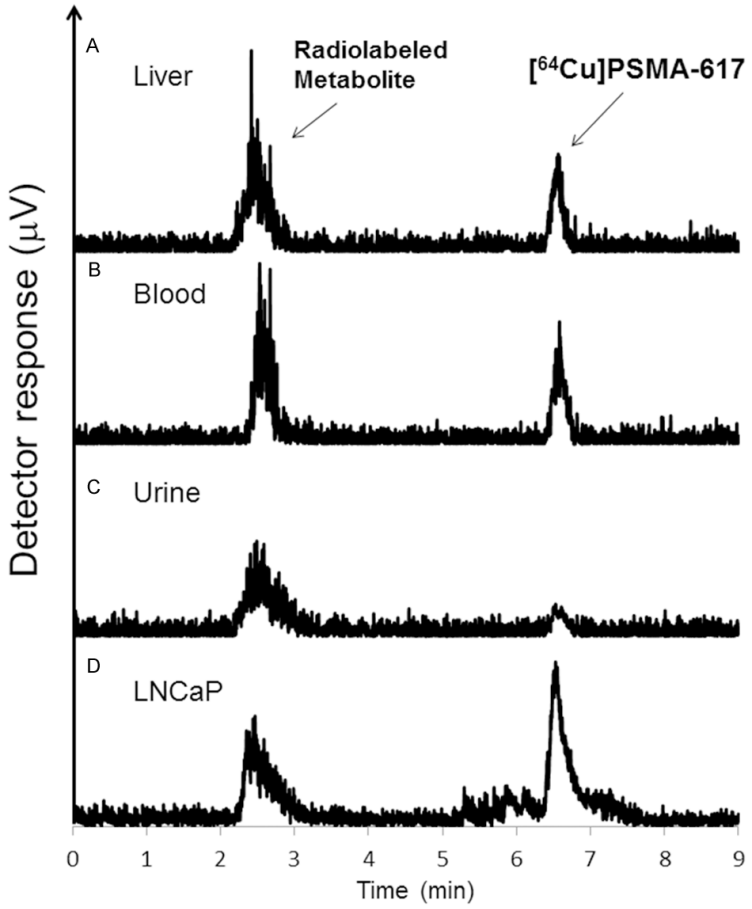

Figure 4. Radio-HPLC chromatograms for in vivo metabolite analysis of the liver (A), blood (B), urine (C), and LNCaP tumor (D) samples at 2 h after the injection of [^{64}Cu]PSMA-617.

activity uptake by LNCaP cells. When PSMA-617 was added to the incubation mixture at a total concentration of 8.56 nM (5.63-13.01 nM, 95% confidence interval), the radioactivity level decreased to 50% of the control cellular uptake. This experiment indicated that [^{64}Cu]PSMA-617 has a high binding affinity for PSMA, and significant specificity for the PSMA-positive LNCaP. It was assumed that the efflux of [^{64}Cu]PSMA-617 might be from the cell surface-bound activity and may be similar to the efflux of ^{68}Ga-labeled PSMA-617 analogs [26].

Metabolite analysis in normal mice and tumor-bearing mice

To investigate the stability of [^{64}Cu]PSMA-617 *in vivo*, metabolite analysis was performed on the mice. One hour after the injection of [^{64}Cu]PSMA-617 into mice, only unchanged [^{64}Cu]PSMA-617 was observed in the blood, liver, and urine. As shown in the radio-HPLC chromatograms (**Figure 4**) of the liver homogenate (A), blood (B), urine (C), and LNCaP tumor (D) at 2 h, the fraction corresponding to unchanged [^{64}Cu]PSMA-617 (t_R = 6.2-6.4 min) had decreased to 28.0% in liver, 20.1% in blood and 5.2% in urine. The polar radiolabeled metabolite (t_R = 2.1-2.8 min) was observed in the HPLC charts for the all analyzed samples. This radiolabeled metabolite may have been a ^{64}Cu-conjugator formed in the liver by ^{64}Cu-transchelation with superoxide dismutase [27]. At 2 h after the injection of [^{64}Cu]PSMA-617, a radiolabeled metabolite was observed with 54.7% in the LNCaP tumor tissues, in addition to the intact form (**Figure 4D**).

PET imaging of normal mice

The biodistribution and pharmacokinetics of [^{64}Cu]PSMA-617 in normal mice were determined by small-animal PET scans (**Figure 5**). **Figure 5A** shows typical PET MIP images of whole mice bodies at several time points following injection of [^{64}Cu]PSMA-617. **Figure 4B** shows [^{64}Cu]PSMA-617 time-activity curves (TACs) of mice for the first 60 min following injection. The injected dosing solution was carried through the vena cava to the heart, which distributed to the whole body. The radioactivity rapidly peaked in the lung, heart and kidneys by 0.5 min, and was subsequently eliminated from these organs. About 20% of the initial uptake remained in the kidneys 60 min after the injection. The radioactivity level in the liver, initially decreased to 1 SUV and remained within the range of 1-2 SUV.

These PET scans enabled visualization of mice livers, kidneys, and urinary bladders. The renal uptake of radioactivity may be partially due to the expression of PSMA in mouse proximal renal tubules [28]. The duodenum, colon, and urinary bladder reportedly express PSMA [28], which probably contributes to the radioactivity

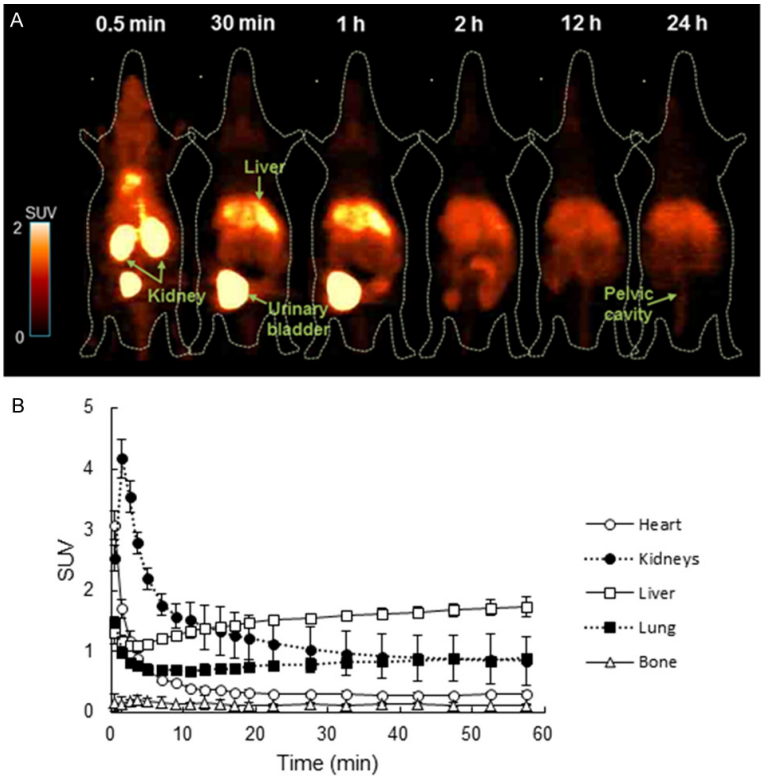

Figure 5. PET study of [^{64}Cu]PSMA-617 in ICR normal mice. MIP images (A) and 60-minute-long TACs (B) for heart, lung, bone, liver, and kidneys were exhibited.

uptake by these tissues to some extent. In addition to the uptake reflecting the PSMA expression, the high uptakes and pharmacokinetics in the kidneys and urinary bladder may reflect a rapid and main excretion route of radioactivity through the kidneys to urine. On the other hand, the low *in vivo* stability of [^{64}Cu]PSMA-617 may mainly contribute to the high radioactivity retained by the liver. Some ^{64}Cu-DOTA ligands are associated with trans-chelation of ^{64}Cu by other proteins endogenous to the liver [29-31].

Ex vivo biodistribution in normal mice

To further investigate its pharmacokinetics, we characterized *ex vivo* distribution of [^{64}Cu]PSMA-617 in mice. **Table 1** shows the uptake of radioactivity in selected organs at 0.5, 1, 2, 12 and 24 h after radioligand injection. At 0.5 h, a high uptake (>3% ID/g) was observed in the lung (4.6 ± 1.1% ID/g), liver (12.7 ± 0.8% ID/g), and kidneys (29.4 ± 12.5% ID/g). After the initial increments, the radioactivity decreased in the liver and kidneys.

The distribution pattern of radioactivity in this experiment was consistent with PET data. The initial renal uptake of radioactivity was highest among all tissues, and decreased to 4.0 ± 0.7% ID/g at 24 h post-injection. In the non-targeted organs with low or no PSMA expression such as the blood, heart, spleen, and pancreas, similarly low levels of radioactivity (<2% ID/g) were retained at 24 h.

PET imaging of tumor-bearing mice

PET imaging study with [^{64}Cu]PSMA-617 was performed on the tumor-bearing mice. PSMA-positive LNCaP cells and PSMA-negative PC-3 cells were implanted into the left and right flanks of mice, respectively. **Figure 6A** shows MIP images taken 2 min, 10 min, 30 min, 60 min, 2 h, and 24 h after radioligand injection. **Figure 6B** shows the TACs of [^{64}Cu]PSMA-617 for the two tumor areas and main organs over the first 60 min following administration. A considerable uptake of radioactivity was observed for the LNCaP tumor area with a definite level within 60 min; low uptake was observed for the PC-3 area. Significant uptakes were also observed in the kidneys and liver, as determined in the TACs. The renal radioactivity in the tumor-bearing mice was much higher than in the normal mice, while the liver uptake for the tumor mice was not significantly different from that of normal mice.

Quantitative analysis of the PET static images revealed that LNCaP uptake at 2 min following administration was 0.67 ± 0.12 SUV. An increased LNCaP uptake was observed at 60 min (0.99 ± 0.26), while a low and stable PC-3 uptake occurred over the same 60 min period (0.15 ± 0.08 SUV at 2 min and 0.14 ± 0.07 SUV at 60 min). The SUV of LNCaP at 2 h was 0.93 ± 0.25, higher than that of PC-3 (0.16 ± 0.09 SUV). A similar result was observed at 24 h (LNCaP: 0.83 ± 0.23 SUV to PC-3: 0.25 ± 0.15 SUV). The LNCaP uptake of [^{64}Cu]PMSA-617

Table 1. Biodistribution (% ID/g) of radioactivity in ICR mice (n = 4) after the injection of [^{64}Cu]PSMA-617

Time (h)	0.5	1	2	12	24
Blood	0.94 ± 0.03	0.9 ± 0.21	0.99 ± 0.29	1.20 ± 0.43	0.93 ± 0.32
Heart	1.86 ± 0.3	1.56 ± 0.12	2.23 ± 0.5	2.56 ± 0.66	2.14 ± 0.59
Duodenum	5.55 ± 0.47	5.81 ± 0.48	6.99 ± 2.56	3.42 ± 0.10	2.58 ± 0.70
Kidneys	29.42 ± 12.51	15.96 ± 3.09	7.27 ±1.17	4.09 ± 0.55	3.95 ± 0.65
Liver	12.65 ± 0.75	11.05 ± 2.12	11.4 ± 1.69	9.51 ± 1.06	9.08 ± 0.57
Lung	4.61 ± 1.05	5.77 ± 0.92	7.19 ± 1.32	5.13 ± 0.66	3.59 ± 0.86
Muscle	0.47 ± 0.16	0.37 ± 0.11	0.45 ± 0.18	0.50 ± 0.15	0.44 ± 0.15
Pancreas	1.20 ± 0.19	1.51 ± 0.33	2.40 ± 0.95	1.58 ± 0.47	1.29 ± 0.21
Spleen	1.18 ± 0.25	1.22 ± 0.42	1.45 ± 0.73	2.59 ± 0.80	1.84 ± 0.51
Stomach	2.51 ± 0.64	3.55 ± 0.23	4.99 ± 1.47	0.74 ± 0.10	1.03 ± 0.44

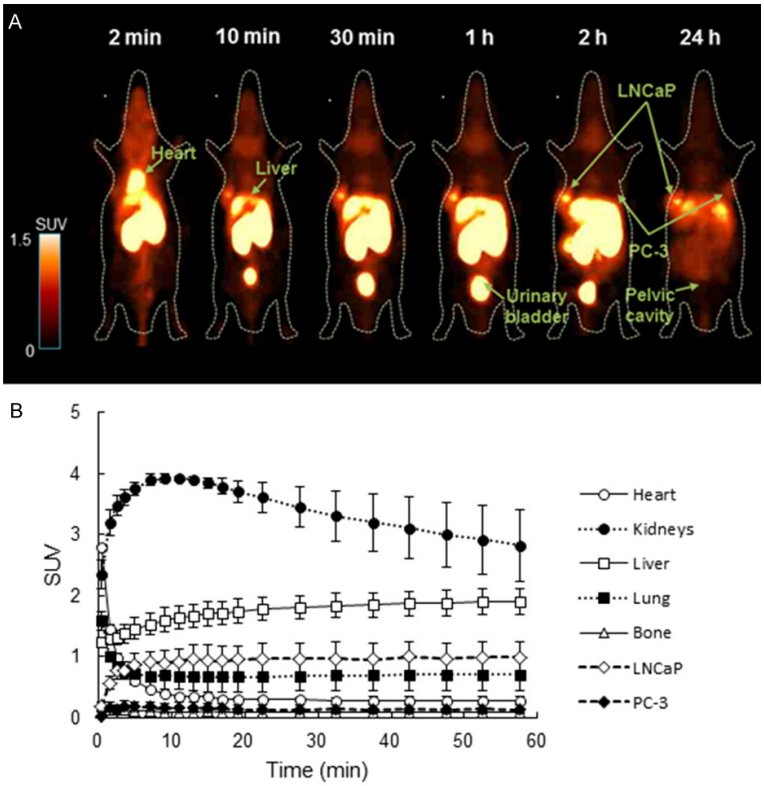

Figure 6. PET study of [^{64}Cu]PSMA-617 in tumor-bearing-mice. MIP images (A) and 60-minute-long TACs (B) of two tumors (LNCaP and PC-3), heart, lung, bone, liver, and kidneys were exhibited.

was higher than the corresponding uptake by PSMA-negative PC-3 at all time points, which confirmed that *in vivo* uptake of radioactivity examined in the LNCaP tumor was PSMA-mediated.

In the PET experiments, non-targeted organs, such as the heart, lung and bone, exhibited low uptake. Within 1 h after the injection of [^{64}Cu] PSMA-617 the renal uptake was greater in the tumor-bearing mice (**Figure 6**) than in the normal mice (**Figure 5**). The putative reason of this result may be that the tumor-derived exosomes containing PSMA accumulated in the kidneys to produce the additional renal uptake in tumor-bearing mice [32]. Twenty-four hours after the injection of this radioligand, radioactivity had largely cleared from the kidneys, producing high target-to-background contrast. This result is favorable for the PET study of tumors. However, we also observed relatively high nonspecific uptake by the liver, which probably caused noisy signal and radiation damage to the subjects.

Immunohistochemical staining

A strong signal of fluorescence was visualized by immunofluorescence staining of the LNCaP tumor and kidney. PSMA was found to express highly in this tumor and kidney slices (**Figure 7**). Contrary to PSMA expression in LNCaP, PSMA expression and fluorescence was not observed in the PC-3 tumor and liver slices. Point-like fluorescence was detected in kidney cortex, but not found in medulla part. This finding may be related to tumor-derived exosomes containing PSMA accumulated in kidney of tumor-bearing mice as mentioned in the above PET study. These results were consistent with the [^{64}Cu]

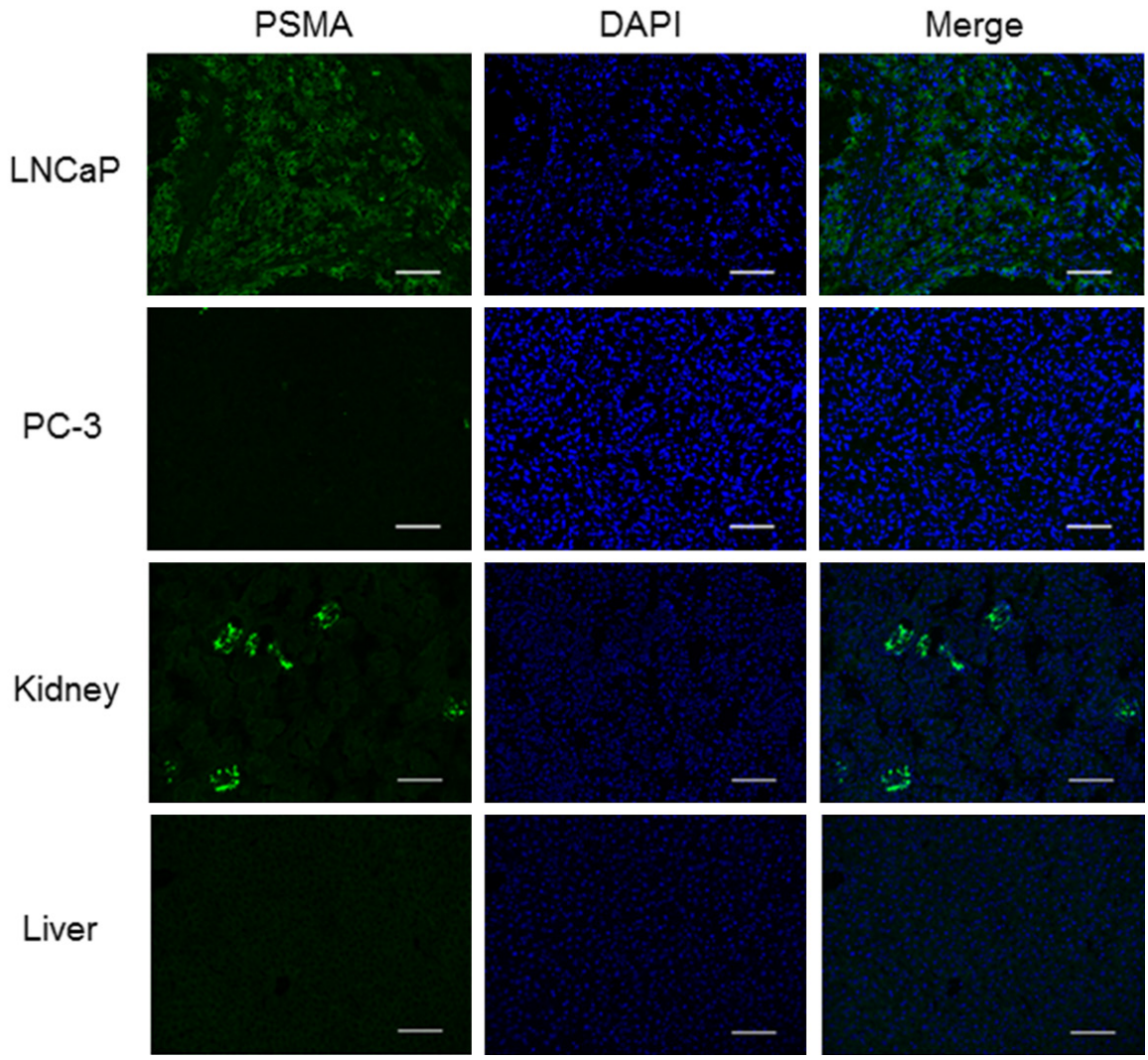

Figure 7. Immunofluorescence staining. PSMA expression is positive in LNCaP tumor and cortex part of kidney tissue sections and negative in PC-3 tumor and liver tissue sections. The cell nuclei were visualized using DAPI. Scale bar: 100 μm.

PSMA-617 PET findings and with the physiological expression of PSMA in the kidney, which demonstrated that focal uptake of [^{64}Cu]PSMA-617 in the LNCaP areas was mainly due to PSMA expression.

The present *in vitro* and *in vivo* evaluation indicated that [^{64}Cu]PSMA-617 could be used to visualize PSMA-positive PCa. PET with [^{64}Cu]PSMA-617 exhibited relatively high tumor-to-normal tissue ratios. For example, the ratios of LNCaP radioactivity to heart and bone radioactivity were 2.9 and 9.3 at 24 h after the injection, respectively. Very little bone uptake was observed, indicating that this radioligand may find application for the detection of PCa metastases, which are preferentially found in bone. As shown by the PET data for normal and tumor-bearing mice, uptake was extremely low in the pelvic cavity 24 h after radioligand injection (**Figures 5A** and **6A**); this characteristic of [^{64}Cu]PSMA-617 is favorable for its clinical use. The detection of lymph metastasis of PCa is based on pelvic lymphadenectomy [30]; low pelvic cavity uptake may enable noninvasive detection of lymph metastasis in this tissue.

[^{64}Cu]PSMA-617 has a shortcoming. This radioligand is not stable *in vivo*. Because of the trans-chelation of ^{64}Cu, a radiolabeled metabolite may be produced and easily accumulated by the liver. Moreover, this radiolabeled metab-

olite was also found in the tumor tissues, which would decrease signals specific to PSMA and increase noisy signals. There was in vivo pharmacokinetic difference between [^{64}Cu]PSMA-617 and [^{68}Ga]PSMA-617. Compared to [^{68}Ga]PSMA-617, [^{64}Cu]PSMA-617 showed a higher liver uptake and slower clearance of radioactivity from the kidneys in the tumor-bearing mice. High liver uptake is a common phenomenon for some ^{64}Cu-DOTA-labeled ligands [27, 29-31]. To improve *in vivo* stability of ^{64}Cu-labeled PSMA-617 ligand, it may be worthwhile to substitute DOTA for other chelators. Conjugating the PSMA ligand to an alternative chelator such as 2-[4,7-bis-(carboxymethyl)-[1,4,7]triazonan-1-yl]acetic acid (NOTA) or 4,8,11-tetraazabicyclo[6.6.2]-hexadecane-4,11-diacetic acid (CB2-TE2A) in place of DOTA reportedly decreases liver uptake. For example, a decreased liver uptake of N-[4,7-bis(carboxymethyl)octahydro-1H-1,4,7-triazonin-1-yl]acetic acid (NODAGA) or CB-TE2A-conjugated PSMA radioligand has been explained by its higher *in vivo* stability [22, 29, 33, 34].

Conclusion

In this study, we synthesized [^{64}Cu]PSMA-617 for the first time, performed the biodistribution, metabolite analysis, and PET studies, and further assessed its usefulness in detecting PSMA-positive PCa. *In vitro* study indicated [^{64}Cu]PSMA-617 was taken into the PSMA-positive LNCaP cells and bound specifically to PSMA. PET scans enabled visualization of PSMA-positive PCa. However, the high liver uptake of radioactivity and slow clearance from kidneys due to [^{64}Cu]PSMA-617 instability *in vivo* may preclude wide application of this radioligand. Change of the DOTA chelator moiety may enable development of more useful ^{64}Cu or ^{67}Cu-labeled PSMA ligands for imaging and targeted radiotherapy.

Acknowledgements

We would like to thank the staff at the National Institute of Radiological Sciences for their help with cyclotron operation, radioisotope production, radiosynthesis, and animal experiments.

Disclosure of conflict of interest

None.

Address correspondence to: Dr. Feng Wang, Department of Nuclear Medicine, Nanjing First Hospital, Nanjing Medical University, Nanjing 210029, China. E-mail: fengwangcn@hotmail.com; Dr. Mingrong Zhang, Department of Radiopharmaceutics Development, National Institute of Radiological Sciences, National Institutes for Quantum and Radiological Science and Technology, Chiba 263-8555, Japan. E-mail: zhang.ming-rong@qst.go.jp

References

[1] Rahib L, Smiyj BD, Aizenberg R, Rosenzweig AB, Fleshman JM, Matrisian LM. Projecting cancer incidence and deaths to 2030: the unexpected burden of thyroid, liver, and pancreas cancers in the United States. Cancer Res 2014; 74: 2913-2921.

[2] Ferlay J, Steliarova-Foucher E, Lortet-Tieulent J, Rosso S, Coebergh JWW, Comber H, Forman D, Bray F. Cancer incidence and mortality patterns in Europe: estimates for 40 countries in 2012. Eur J Cancer 2013; 49: 1374-1403.

[3] Ghosh A, Heston WD. Tumor target prostate specific membrane antigen (PSMA) and its regulation in prostate cancer. J Cell Bio Chem 2004; 91: 528-539.

[4] Silver DA, Pellicer I, Fair WR, Heston WD, Cordon-Cardo C. Prostate-specific membrane antigen expression in normal and malignant human tissues. Clin Cancer Res 1997; 3: 81-85.

[5] Dumas F, Gala JL, Berteau P, Brasseur F, Eschwége O, Paradis V, Lacour B, Philippe M, Loric S. Molecular expression of PSMA mRNA and protein in primary renal tumors. Int J Cancer 1999; 80: 799-803.

[6] Gala JL, Loric S, Guiot Y, Denmeade SR, Gady A, Brasseur F, Heusterspreute M, Eschwège P, De Nayer P, Van Cangh P, Tombal B. Expression of prostate- specific membrane antigen in transitional cell carcinoma of the bladder: prognostic value? Clin Cancer Res 2000; 6: 4049-4054.

[7] Chang SS, Reuter VE, Heston WD, Bander NH, Grauer LS, Gaudin PB. Five different anti-prostate-specific membrane antigen (PSMA) antibodies confirm PSMA expression in tumor-associated neovasculature. Cancer Res 1999; 59: 3192-3198.

[8] Sodee DB, Malguria N, Faulhaber P, Resnick MI, Albert J, Bakale G. ProstaScint® imaging findings in 2154 patients with prostate cancer. Urology 2000; 56: 988-993.

[9] Vallabhajosula S, Kuji I, Hamacher KA, Konishi S, Kostakoglu L, Kothari PA, Milowski MI, Nanus DM, Bander NH, Goldsmith SJ. Pharmacokinetics and biodistribution of ^{111}In- and ^{177}Lu-labeled J591 antibody specific for pros-

tate-specific membrane antigen: prediction of ^{90}Y-J591 radiation dosimetry based on ^{111}In or ^{177}Lu. J Nucl Med 2005; 46: 634-641.

[10] Reske SN, Blumstein NM, Neumaier B, Gottfried HW, Finsterbusch F, Kocot D, Möller P, Glatting G, Perner S. Imaging prostate cancer with ^{11}C-choline PET/CT. J Nucl Med 2006; 47: 1249-1254.

[11] Schuster DM, Votaw JR, Nieh PT, Yu W, Nye JA, Master V, Bowman FD, Issa MM, Goodman MM. Initial experience with the radiotracer anti-1-amino-3-^{18}F-fluorocyclobutane-1-carboxylic acid with PET/CT in prostate carcinoma. J Nucl Med 2007; 48: 56-63.

[12] Machulkin AE, Ivanekov YA, Aladinskaya AV, Veselov MS, Aladinskiy VA, Beloglazkina EK, Koteliansky VE, Shakhbazyan AG, Sandulenko YB, Majouga AG. Small-molecule PSMA ligands. Current state, SAR and perspectives. Drug Target 2016; 24: 679-93.

[13] Kozikowski AP, Nan F, Conti P, Zhang J, Ramadan E, Bzdega T, Wroblewska B, Neale JH, Pshenichkin S, Wroblewski JT. Design of remarkably simple, yet potent urea-based inhibitors of glutamate carboxypeptidase II (NAALADase). J Med Chem 2001; 44: 298-301.

[14] Kozikowski AP, Zhang J, Nan F, Petukhov PA, Grajkowska E, Wroblewski JT, Yamamoto T, Bzdega T, Wroblewska B, Neale JH. Synthesis of Urea-based inhibitors as active site probes of glutamate carboxypeptidase II: efficacy as analgesic agents. J Med Chem 2004; 47: 1729-1738.

[15] Foss CA, Mease RC, Fan H, Wang Y, Ravert HT, Dannals RF, Olszewski RT, Heston WD, Kozikowski AP, Pomper MG. Radiolabeled small-molecule ligands for prostate-specific membrane antigen: in vivo imaging in experimental models of prostate cancer. Clin Cancer Res 2005; 11: 4022-4028.

[16] Mease RC, Dusich CL, Foss CA, Ravert HT, Dannals RF, Seidel J, Prideaux A, Fox JJ, Sgouros G, Kozikowski AP, Pomper MG. N-[N-(S)-1,3-dicaboxypropyl]carbamoyl]-4-[^{18}F]fluorobenzyl-L-cysteine, [^{18}F]DCFBC: a new imaging probe for prostate cancer. Clin Cancer Res 2008; 14: 3036-3043.

[17] Benešová M, Schäfer M, Bauder-Wüst U, Afshar-Oromieh A, Kratochwil C, Mier W, Haberkorn U, Kopka K, Eder M. Preclinical evaluation of a tailor-made DOTA-Conjugated PSMA inhibitor with optimized linker moiety for imaging and endoradiotherapy of prostate cancer. J Nucl Med 2015; 56: 914-920.

[18] Benešová M, Bauder-Wüst U, Schäfer M, Klika KD, Mier W, Haberkorn U, Kopka K, Eder M. Linker modification strategies to control the prostate-specific membrane antigen (PSMA)-targeting and pharmacokinetic properties of DOTA-conjugated PSMA inhibitors. J Med Chem 2016; 59: 1761-1775.

[19] Afshar-Oromieh A, Hetzheim H, Kratochwil C, Benesova M, Eder M, Neels OC, Eisenhut M, Kübler W, Holland-Letz T, Giesel FL, Mier W, Kopka K, Haberkorn U. The theranostic PSMA ligand PSMA-617 in the diagnosis of prostate cancer by PET/CT: biodistribution in humans, radiation dosimetry, and first evaluation of tumor lesions. J Nucl Med 2015; 56: 1697-1705.

[20] Elisabeth E, Fuente A de la, Kürpig S, Roesch F, Essler M. ^{44}Sc and ^{177}Lu-labeling of DOTA-PSMA DKFZ-617 for dosimetry and therapy of prostate cancer. J Label Comp Radiopharm 2015; 58: S353.

[21] Delker A, Fendler WP, Kratochwil C, Brunegraf A, Gosewisch A, Gildehaus FJ, Tritschler S, Stief CG, Kopka K, Haberkorn U, Bartenstein P, Böning G. Dosimetry for 177Lu-DKFZ-PSMA-617: a new radiopharmaceutical for the treatment of metastatic prostate cancer. Eur J Nucl Med Mol Imaging 2016; 43: 42-51.

[22] Gourni E, Canovas C, Goncalves V, Denat F, Meyer PT, Maecke HR. (R)-NODAGA-PSMA: a versatile precursor for radiometal labeling and nuclear imaging of PSMA-positive tumors. PLoS One 2015; 10: e0145755.

[23] Wadas TJ, Wong EH, Weisman GR, Anderson CJ. Coordinating radiometals of copper, gallium, indium, yttrium, and zirconium for PET and SPECT imaging of disease. Chem Rev 2010; 110: 2858-2902.

[24] Ohya T, Nagatsu K, Suzuki H, Fukada M, Minegishi K, Hanyu M, Fukumura T, Zhang MR. Efficient preparation of high-quality ^{64}Cu for routine use. Nucl Med Biol 2016; 43: 685-691.

[25] Yang M, Loda M, Sytkowski AJ. Identification of genes expressed differentially by LNCaP or PC-3 prostate cancer cell lines. Cancer Res 1998; 58: 3732-3735.

[26] Schäfer M, Bauder-Wüst U, Leotta K, Zoller F, Mier W, Haberkorn U, Eisenhut M, Eder M. A dimerized urea-based inhibitor of the prostate-specific membrane antigen for 68Ga-PET imaging of prostate cancer. EJNMMI Res 2012; 2: 23.

[27] Bass LA, Wang M, Welch MJ, Anderson CJ. In vivo transchelation of copper-64 from TETA-Octreotide to superoxide dismutase in rat liver. Bioconjugate Chem 2000; 11: 527-532.

[28] Kinoshita Y, Kuratsukuri K, Landas S, Imaida K, Rovito PM Jr, Wang CY, Haas GP. Expression of prostate-specific membrane antigen in normal and malignant human tissues. World J Surg 2006; 30: 628-636.

[29] Boswell CA, Sun X, Niu W, Weisman GR, Wong EH, Rheingold AL, Anderson CJ. Comparative in vivo stability of copper-64-labeled cross-bridged and conventional tetraazamacrocyclic complexes. J Med Chem 2004; 47: 1465-1474.

[30] Neumann PZ, Sass-Kortsak A. The state of copper in human serum: evidence for an amino acid-bound fraction. J Clin Invest 1967; 46: 646-658.
[31] Wang H, Chen X. Visualization of copper metabolism by $^{64}CuCl_2$-PET. Mol Imaging Biol 2012; 14: 14-16.
[32] Mizutani K, Terazawa R, Kameyama K, Kato T, Horie K, Tsuchiya T, Seike K, Ehara H, Fujita Y, Kawakami K, Ito M, Deguchi T. Isolation of prostate cancer-related exosomes. Anticancer Res 2014; 34: 3419-3423.
[33] Heidenreich A, Bastian PJ, Bellmunt J, Bolla M, Joniau S, van der Kwast T, Mason M, Matveev V, Wiegel T, Zattoni F, Mottet N; European Association of Urology. EAU guidelines on prostate cancer. Part 1: screening, diagnosis, and local treatment with curative intent-update 2013. Eur Urol 2014; 65: 124-137.
[34] Banerjee SA, Pullambhatla M, Foss CA, Nimmagadda S, Ferdani R, Anderson CA, Mease RC, Pomper MG. ^{64}Cu-labeled inhibitors of prostate-specific membrane antigen for PET imaging of prostate cancer. J Med Chem 2014; 57: 2657-2669.